ISSN 1392–1320 MATERIALS SCIENCE (MEDŽIAGOTYRA). Vol. 17, No. 4 2011

# Aqueous Sol-Gel Synthesis Methods for the Preparation of Garnet Crystal Structure Compounds

**Aivaras KAREIVA** *

*Department of General and Inorganic Chemistry, Vilnius University, Naugarduko 24, LT-03225 Vilnius, Lithuania*

crossref http://dx.doi.org/10.5755/j01.ms.17.4.782

*Received 15 September 2011; accepted 12 October 2011*

In the present review, the usefulness of aqueous sol-gel processes in the synthesis of garnet crystal structure compounds is discussed. The processing and characterization of yttrium aluminium garnet (YAG), lanthanide-doped YAG, lanthanide aluminium and gallium garnet materials, mixed-metal garnets and garnets containing silicon are described. The synthesis of garnet materials comprising nanoscale architectures is also discussed.
*Keywords*: sol-gel, water-based, garnets, nanoparticles.

## 1. INTRODUCTION

Yttrium aluminium garnet ($Y_3Al_5O_{12}$, YAG) based materials adopt the cubic garnet structure and are widely used in advanced optical technologies since YAG doped with a transition metal or lanthanide element exhibits outstanding luminescence properties [1]. Namely, YAG can withstand harsh conditions implied by high energy excitations due to an important damage threshold and show emissions of wavelength lying near infrared range to the UV range of the electromagnetic spectrum. These features have made YAG a relevant material as window for a variety of lamps, for fiber-optic telecommunication systems, for cathode-ray tubes, field emission displays, plasma display panel, light-emitting diodes, electroluminescent and medical applications [1 – 4].

All mentioned properties of YAG based oxide ceramics are highly sensitive not only to the changes in dopant composition or host stoichiometry, but also to the processing conditions, which are very much responsible for the crystallinity, crystal shape, crystal size, crystal size distribution and phase purity of the resulting powders. In order to prepare these oxides, the solid state reaction method is still utilized because of its lower manufacturing cost and simpler preparation process. However, this method, in general, requires the calcination temperature higher than 1000 °C to eliminate the unreacted starting oxides and to obtain the final product of a single phase. In order to overcome these inevitable disadvantages arising from the solid state reaction, some other methods have been also suggested. Over the last few decades, the sol-gel techniques have been used to prepare a variety of mixed-metal oxides, nanomaterials and nanoscale architectures, nanoporous oxides, organic-inorganic hybrids [5 – 7].

Electronic materials now represent one of the largest manufacturing sectors in the world. One challenge for the high end of the market is the development of alternative synthesis technologies that are not just "greener" but provide environmentally benign processes [8, 9]. In this paper we present results of a systematic study of environmentally friendly an aqueous sol-gel synthetic approach to micro- and nanosized selected garnet crystal structure compounds. The results are presented herein.

## 2. YTTRIUM ALUMINIUM GARNET (YAG)

The first sol-gel syntheses of yttrium aluminium garnet using a water based routes were described by Vaqueiro and Lopez-Quintela [10] and Veith et al. [11]. In the citrate sol-gel process [10] metal nitrates were selected as starting materials. However, in the glycolate sol-gel route [11] the metal acetates were used. It has been demonstrated that using the citrate and glycolate sol-gel processes the pure polycrystalline YAG samples were obtained at 1000 °C, which is much lower temperature than using the solid state reaction method. The sol-gel process offers considerable advantages such as better mixing of the starting materials and excellent chemical homogeneity in the final product. Moreover, the molecular level mixing and the tendency of partially hydrolyzed species to form extended networks facilitate the structure evolution thereby lowering the crystallization temperature. The evaluated synthetic technique to YAG using acetate-glycolate intermediate illustrates the simplicity and superior potential of proposed method. This innovative approach offers a feasible way to obtain a new nanoscaled ceramic materials having garnet structure with well-established application as laser hosts.

The influence of nineteen sol-gel processing variables on the formation of YAG has been investigated. Effects of different fabrication parameters on the phase purity and morphological properties of the compounds were studied by energy-dispersive spectrometry (EDS), X-ray powder diffraction (XRD) analysis and scanning electron microscopy (SEM). The parameters of the sol-gel processing such as pH of starting solution, concentration and nature of complexing ligand, temperature and duration of gelation, powder rehomogenization during annealing, duration and temperature of the final heat treatment were found to be the most significant. For the evaluation and verification of the experimental results the Brandon's model of a multiple regression was successfully used [12].

* Corresponding author. Tel.: +370-5-2193110fax.: +370-5-2330987.
E-mail address: *aivaras.kareiva@chf.vu.lt* (A. Kareiva)

Fig. 1 shows the XRD spectra of the YAG samples synthesized using different pH values in the sol-gel process.

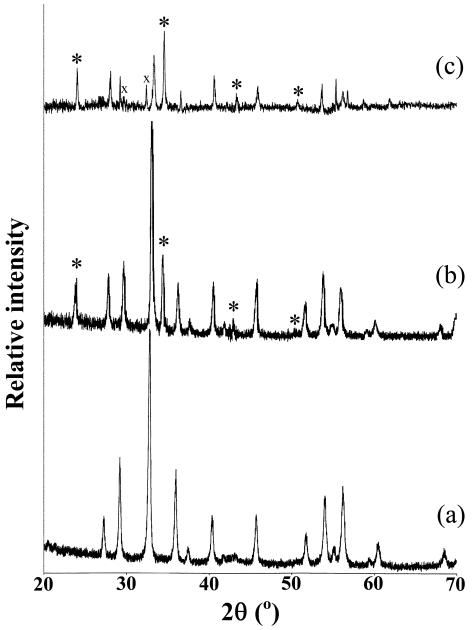


**Fig. 1.** XRD patterns of the YAG samples synthesized using different pH values in the sol-gel process: a – 5.5; b – 7.0; c – 3.5. The impurity phases are marked: YAP (*) and YAM ($^{x}$)

Monophasic garnet samples were obtained when the pH value of the sols was maintained between 5.5 and 6.5. The X-ray diffraction pattern of the sample synthesized at pH = 7.0 (Fig. 1, b) looks similar to the previous one; however, the formation of a significant amount of perovskite yttrium aluminate ($YAlO_3$, YAP) as an impurity phase was also identified (marked with asterisks). So, if the pH of solutions in the sol-gel process is not optimized possibly precipitates are formed during the condensation reactions instead of a homogeneous gel network are formed. The eight most significant parameters in the sol-gel preparation of YAG were found to be pH, concentration and nature of complexing ligand, temperature and duration of the hydrolysis-condensation reactions during gelation, powder rehomogenization during annealing, duration and temperature of the final heat treatment. The influence of most significant parameters was evaluated using this mathematical model. For this purpose the initial data set has been split up into three regions, and the models for each of those regions were built. The results obtained from each model were found to be in a good agreement with experimental ones. The computational model has been constructed that provides quantitative agreement of YAG formation reaction mechanisms with the experimental data of process parameters and desired structural, morphological and physical properties of the final ceramic material [13 – 15].

Nanocrystalline YAG was synthesized by means of a modified glycolate sol-gel method in an aqueous media [16]. The monophasic YAG having the crystallites size of 26 nm was obtained at 800 °C. YAG fibres have been also produced from an aqueous sol-gel route, using a commercially available alumina sol combined with yttria sol containing nitrate counterions [17].

## 3. LANTHANIDE-DOPED YAG

In the study [18] the synthesis of polycrystalline holmium- and neodymium-doped (5 mol %) yttrium aluminium garnet (YAG) by the glycolate sol-gel process was described. The sensitivity of the magic angle spinning (MAS) $^{27}$Al NMR chemical shifts towards the coordination state of Al (III) was used for identifying the different phases and coordination states of Al centres in Y-Al-Ho-O and Y-Al-Nd-O precursor gels (Fig. 2).

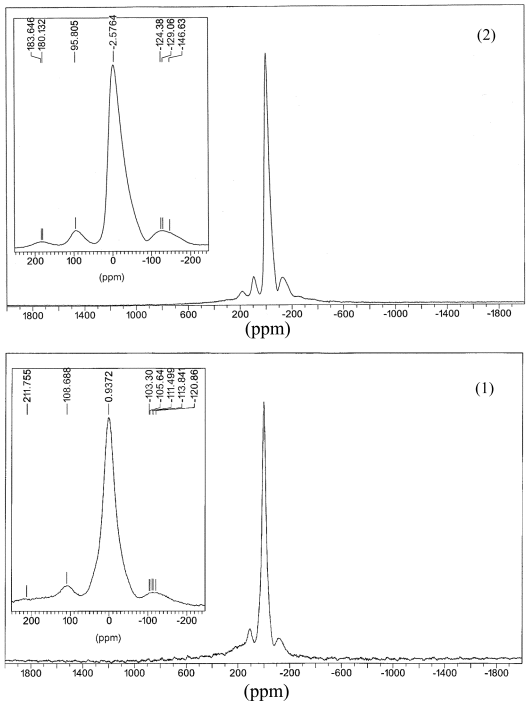


**Fig. 2.** $^{27}$Al MAS NMR spectra of the Y-Al-Ho-O (1) and Y-Al-Nd-O (2) precursor gels

It is known, that the solid-state structure of $Y_3Al_5O_{12}$ consists of a network of four- and six-fold coordinated aluminium atoms. The yttrium atoms reside in the dodecahedral interstices formed by the corner-sharing arrangement of the $AlO_4$ and $AlO_6$ polyhedra. As seen, the major resonance in the $^{27}$Al NMR spectra of the unheated gels (δ 0.937 for the Y-Al-Ho-O gel and δ –2.576 for the Y-Al-Nd-O gel) occurs in the position of octahedrally coordinated Al. Much smaller features at ca. 96 ppm – 108 ppm indicate a small proportion of the Al in the initial gels is located in tetrahedral sites. Moreover, a comparison of the intensity of the signals due to $AlO_4$ and $AlO_6$ units in the gels obtained, suggests the initial gel structures to be very similar.

The lattice parameters of the doped YAG samples were obtained (Table 1). As seen, from the refined lattice parameters, the particles of oxides do not exhibit a lattice expansion with incorporation of certain amount of dopant in YAG ceramics. Consequently, the unit cell volume remains nearly constant as well. Later on, the Ce- and Er-doped YAG samples were also synthesized using the same aqueous sol-gel technique and investigated [19, 20].

**Table 1.** Lattice parameters of rare-earth doped $Y_3Al_5O_{12}$

| Dopant | Lattice parameters | |
|---|---|---|
| | $a$ (Å) | Volume (Å$^3$) |
| – | 12.009 | 1731.9 |
| $Ho^{3+}$ | 12.015 | 1734.5 |
| $Nd^{3+}$ | 12.013 | 1733.6 |

In the practical applications as luminescence activator $Nd^{3+}$ plays very important role. Therefore, several successful attempts to prepare Nd-doped YAG using aqueous sol-gel technique were reported by several groups [21 – 24]. The evident influence of the grain size on the luminescence of $Nd^{3+}$ ions has been observed by Hreniak et al. [21, 22]. High-resolution absorption spectra of the powders [24] showed that a higher absorption cross-section of glycolate-derived powders is due to $Nd^{3+}$–$Nd^{3+}$ ion pairing, which leads to the quenching of photoluminescence.

A new sol-gel pyrolysis method for the preparation of large-scale nanocrystalline $Y_3Al_5O_{12}:Ce^{3+}$ has been suggested by Taiwanese scientists [25]. By using metal nitrates and oxides as the starting materials, YAG:$Re^{3+}$ (Re = Ce, Sm, Tb) powder phosphors were prepared by solid-state, coprecipitation and citrate sol-gel methods [26, 27]. Although the citrate sol-gel method can produce relatively homogeneous phosphor particles at lower temperature, its emission intensity is not as high as those from the solid-state- and coprecipitation-derived phosphors, possibly due to the contamination of carbon impurities introduced by the citric acid from the starting materials in the citrate sol-gel method. Single-phase Ce-doped yttrium aluminium garnet samples have been synthesized by an aqueous sol-gel method at 1000 °C in the whole doping range (from 0 mol % up to 10 mol % of Ce). However, it was determined that with increasing synthesis temperature up to 1300 °C the phase purity of synthesis products depends on the concentration of dopant. At low concentration of cerium the YAG samples were found to be monophasic, but starting from 4 mol % of Ce the XRD patterns of YAG:Ce annealed at 1300 °C contained additional diffraction lines attributable to the $CeO_2$ phase [28, 29]. Interestingly, almost identical surface microstructure and particle size were observed for all Ce-doped YAG samples independently on the concentration of dopant and annealing temperature. The transmission electron microscope image of the representative YAG sample is shown in Fig. 3.

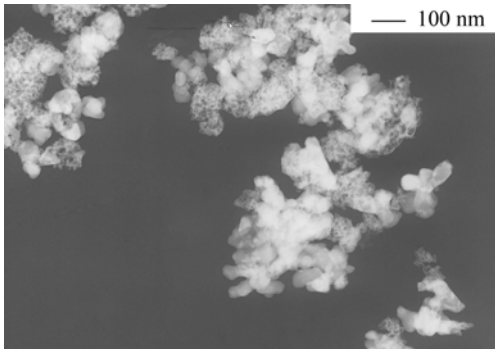


**Fig. 3.** TEM micrograph of $Y_3Al_5O_{12}:Ce$ sample with 5 mol % of Ce and prepared at 1000 °C. Magnification ×75000

The formation of aggregates of primary particles is evident. Fig. 4 shows the emission spectra of $Y_3Al_5O_{12}:Ce$ nanocrystallites.

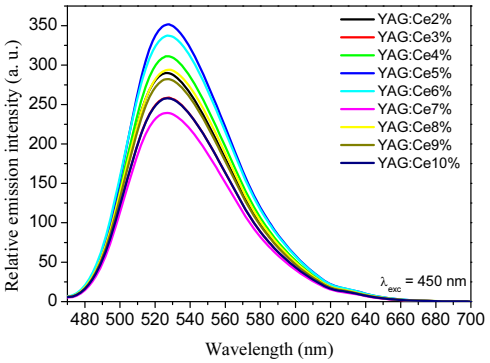


**Fig. 4.** Emission ($\lambda_{ex} = 450$ nm) spectra of $Y_3Al_5O_{12}:Ce$ nanocrystallites synthesized by sol-gel technique and annealed at 1300 °C

As depicted, the position of the broad emission band is almost independent of the Ce concentration and shows as full width at half maximum of about 70 nm. This quite symmetric photoluminescence peak at around 530 nm is assigned to the $5d^1$ ($^2A_{1g}$) → $4f^1$ ($^2F_{5/2}$ and $^2F_{7/2}$) transitions of $Ce^{3+}$. Evidently the highest emission intensity possesses the YAG samples containing 5 mol % and 6 mol % of Ce. $Eu^{3+}$ doped YAG nanophosphors and thin films also have potential for application in field emission devices. Europium-ion doped YAG samples were prepared by citrate sol-gel and sol-gel pyrolysis methods [30, 31]. Interestingly, the emission intensity of well dispersed YAG:$Eu^{3+}$ nanoparticles was found to be much stronger than that of the bulk samples. The properties of YAG:$Eu^{3+}$ nanoparticles can be rationalized by considering numerous surface states due to the large surface area to volume ratio of the nanoparticles.

In view of the improvement of luminescence properties of YAG phosphors, the way of double activation in the host lattice could be successfully used [32 – 34]. Usually, the double incorporation of different lanthanide ions into host crystalline lattice modifies the luminescence spectrum due to the formation of new emission centers.

## 4. LANTHANIDE ALUMINIUM AND GALLIUM GARNET MATERIALS

To obtain yttrium-gallium garnet ($Y_3Ga_5O_{12}$, YGG) a simple “chimie douce” method has also been developed [35, 36]. A schematic diagram of the processing steps involved in the sol-gel synthesis of the $Y_3Ga_5O_{12}$ is shown in Fig. 5. This sol-gel method yielded excellent starting gel precursor for the fabrication of YGG phase, which could be used as host material for optical applications. The XRD pattern of Y-Ga-O gel was recorded in the region of $2\theta = 20° – 60°$ (Fig. 6). The diffraction pattern of the powders obtained is broad due to the amorphous character of the product synthesized. If the conditions of the sol-gel process are not optimized, partial crystallization of initial metal salts (acetates, nitrates or tartrates) may occur. However, no peaks due to insignificant crystallization of these salts or crystallization of any undesired or contaminating phase could be identified.

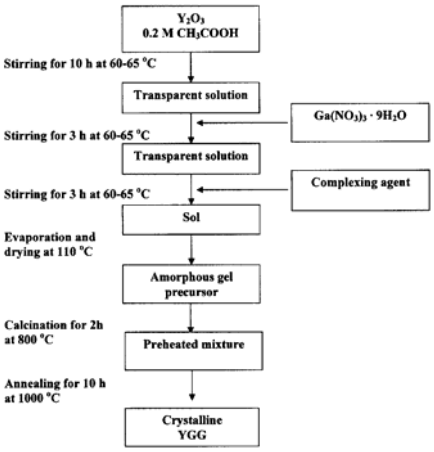


**Fig. 5.** Scheme of the steps involved in the sol-gel process used for the preparation of $Y_3Ga_5O_{12}$ ceramics

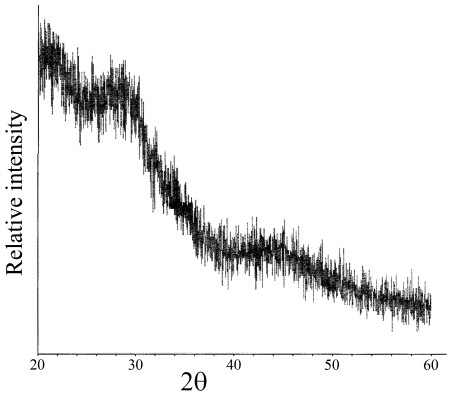


**Fig. 6.** X-ray diffraction pattern of the Y-Ga-O precursor gel

The data from XRD analysis clearly show the individuality of the synthesized precursors. The X-ray diffraction pattern of the ceramic sample sintered for 10 h at 1000 °C (Fig. 7) shows the formation of monophasic $Y_3Ga_5O_{12}$ phase.

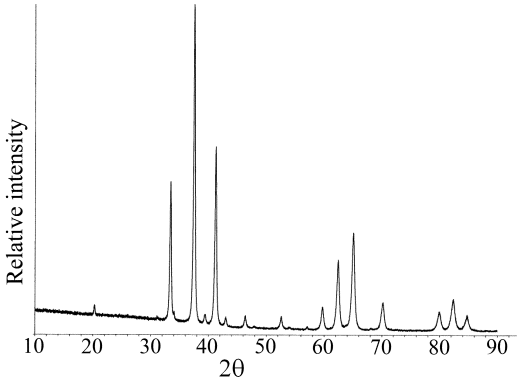


**Fig. 7.** X-ray diffraction pattern of the YGG sample synthesized at 1000 °C

Lutetium gallium garnet ($Lu_3Ga_5O_{12}$, LUGG) was also synthesized by the same aqueous sol-gel process [37]. The X-ray diffraction patterns for the calcined gel powders and sintered for 10 h at 1000 °C and 1200 °C are shown in Fig. 8. According to XRD analysis fully crystallized single-phase oxides $Lu_3Ga_5O_{12}$ with well pronounced garnet crystal structure have formed.

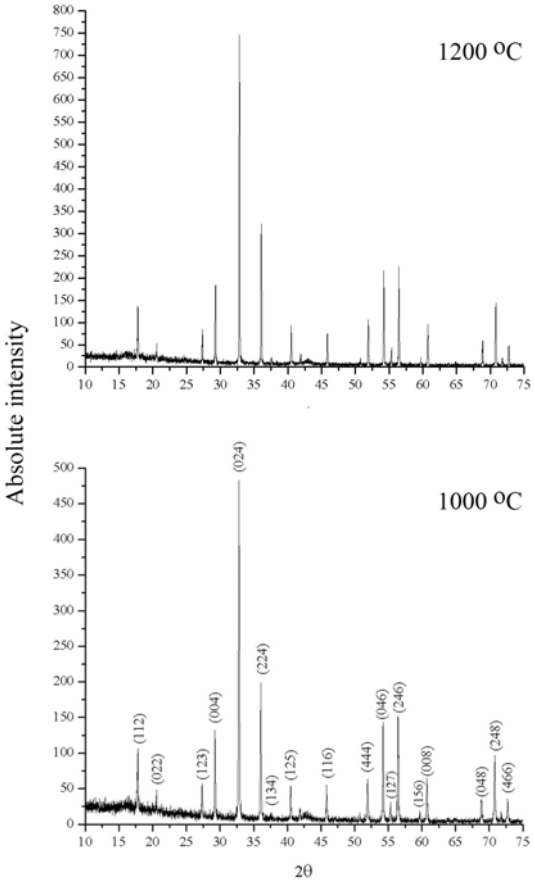


**Fig. 8.** X-ray diffraction patterns of $Lu_3Ga_5O_{12}$ ceramic samples synthesized at different temperatures

As seen, all single lines are indexed, and no unindexed lines could be observed. The most intensive lines are (024) – 100 %, (224) – 39.0 %, and (246) – 37.2 %. Thus, the XRD data confirm $Lu_3Ga_5O_{12}$ to be the only crystalline component already after annealing at 1000 °C. No further significant crystallization with increasing annealing temperature was observed. The lattice parameters of the synthesized LUGG samples were obtained from the diffraction spectra by fitting the peaks of identified reflections. The determined cubic lattice parameters and cell volume for the $Lu_3Ga_5O_{12}$ samples synthesized at 1000 °C were found to be $a = 12.282(3)$ Å and $V = 1852.7(5)$ Å$^3$, respectively.

A sol-gel method based on in-situ generation of mixed-metal chelates by complexing metal ions with ethane-1,2-diol or citric acid in an aqueous media has been elaborated to prepare lanthanide-ion containing garnets, $Gd_3Al_5O_{12}$ (GDAG), $Tb_3Al_5O_{12}$ (TBAG), $Dy_3Al_5O_{12}$ (DYAG), $Ho_3Al_5O_{12}$ (HOAG), $Er_3Al_5O_{12}$ (ERAG), $Tm_3Al_5O_{12}$ (TMAG), $Yb_3Al_5O_{12}$ (YBAG) and $Lu_3Al_5O_{12}$ (LUAG) [38 – 42]. However, the XRD patterns also revealed that during calcination of La-Al-O, Ce-Al-O, Pr-Al-O and Nd-Al-O precursor gels at 800 °C – 1200 °C no formation of garnet structure compounds ($La_3Al_5O_{12}$ (LAAG), $Ce_3Al_5O_{12}$ (CEAG), $Pr_3Al_5O_{12}$ (PRAG), $Nd_3Al_5O_{12}$ (NDAG)) were observed [38, 41, 43, 44]. Thus, rare earth aluminium garnets are thermodynamically stable with RE = Gd – Lu. Garnet structures with larger rare earth ions (La – Eu), perhaps, are metastable, in favour of the competing perovskite type. It is interesting to note that

europium aluminium garnet (EAG) was synthesized for the first time by an aqueous sol-gel process and subsequent thermal annealing at 800 °C – 850 °C [45]. Fig. 9 shows the XRD patterns of samples which were prepared at different temperatures for 30 h from the preheated gel (600 °C).

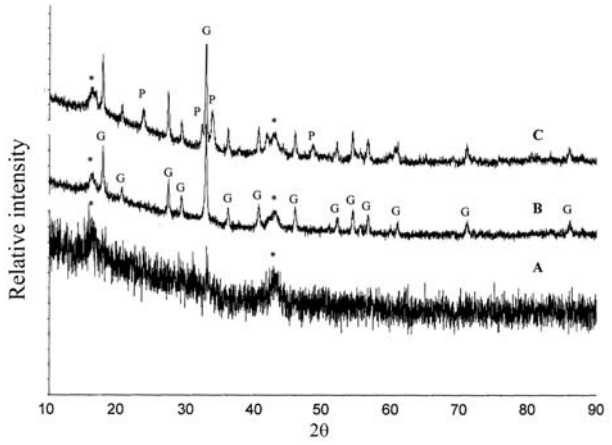


**Fig. 9.** X-ray diffraction patterns of $Eu_3Al_5O_{12}$ annealed 825 °C (A), 835 °C (B) and 850 °C (C). P – perovskite phase; G – garnet phase; * – reflections from sample holder

Evidently, the XRD pattern of Eu-Al-O precursor gel annealed at 835 °C contains diffraction lines which could be assigned to the garnet phase. The results of the Rietveld refinement are presented in Table 2.

**Table 2.** Results of the Rietveld refinement for $Eu_3Al_5O_{12}$

| | |
|---|---|
| Formula | $Eu_3Al_5O_{12}$ |
| Molar weight | 782.79 g/mol |
| Crystal system, Z | cubic, 16 |
| Space group | Ia $\bar{3}$d |
| Lattice parameter | 12.140(1) Å |
| Wave length | 0.7093 Å |
| Angle range | $5° \le 2\theta \le 60°$ |
| Step width | 0.01° |
| Independent reflections | 118 |
| Effective reflections | 65 |
| Parameters | 24 |
| Structure parameters | 7 |
| $R_{Bragg}$ | 6.83 % |
| $R_p$ | 7.14 % |
| $R_{wp}$ | 9.48 % |
| $R_{exp}$ | 6.61 % |

The synthesis of single phase EAG was successfully performed in the temperature region around 825 °C – 835 °C. Treatments at higher temperatures yielded XRD patterns related with perovskite structures. The structure refinement on EAG revealed the well-known cubic garnet structure with $a$ = 12.140(1) Å.

## 5. MIXED-METAL GARNETS

Garnets of type $Y_3Al_{5-y}Ga_yO_{12}$ ($0 \le y \le 5$) (YAGG) and $Y_3Sc_{5-y}Ga_yO_{12}$ ($0 \le y \le 5$) (YSGG) are of special industrial interest, due to their application as laser hosts. Recently a few reports have been published on the synthesis and characterization of single crystals of YAGG and YSGG. On the other hand, the sinterability and microstructal evolution of new mixed-metal $Y_3Sc_xAl_{5-x-y}Ga_yO_{12}$ ($0 \le x, y \le 5$) (YSAGG) powders synthesized by an aqueous sol-gel process were also investigated [46 – 55]. The X-ray diffraction pattern for the $Y_3Sc_{2.5}Ga_{2.5}O_{12}$ sample is shown in Fig. 10.

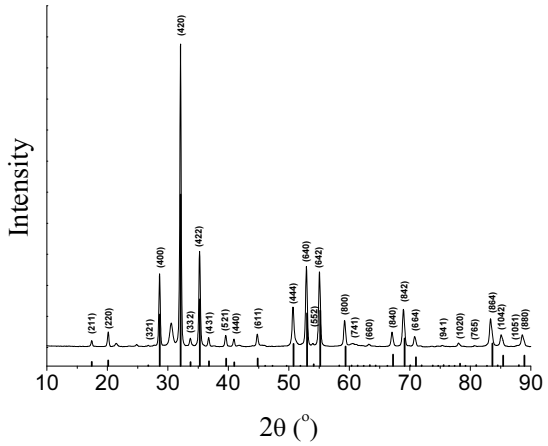


**Fig. 10.** X-ray diffraction pattern of $Y_3Sc_{2.5}Ga_{2.5}O_{12}$ ceramic samples synthesized at 1000 °C. The vertical lines represent the XRD pattern of $Y_3Sc_{1.43}Ga_{3.57}O_{12}$ [PDF 77-1063]

According to XRD analysis fully crystallized oxide $Y_3Sc_{2.5}Ga_{2.5}O_{12}$ with well pronounced garnet crystal structure has formed. As seen, almost all single lines are indexed, and only three unindexed lines at $2\theta \approx$ 21.4, 24.8 and 30.5 could be observed. The most intensive lines are (420) – 100 %, (422) – 32.2 %, and (640) – 27.4 %. The morphological properties of synthesized ceramics were characterized by SEM and TEM measurements. Fig. 11 shows surface features of the representative YSGG sample. As seen, the synthesis product consists of clustered nanograins made up of several tiny crystallites with a defined structure. The SEM micrographs show that the YSGG solids are composed of spherical grains. Individual particles seem to be nearly nano-sized crystals with an average particle size less than 100 nm. Moreover, the SEM images also show a sinter-neck of few nano-YSGG particles which have different orientation to each other. Very well pronounced agglomeration of the nanoparticles indicates a good connectivity between the grains. The TEM investigations once again confirmed high quality of synthesis product. The analogous conclusions from TEM measurements could be drawn, as was indicated by SEM investigations. The TEM image of the YSGG sample is shown in Fig. 12.

As seen from figure, the TEM image of YSGG sample again revealed agglomerated grains. The clustering tendency of the particles in the sol-gel synthesis may be due to the decomposition (> 900 °C) of yttrium oxycarbonate or the traces of the 'unburned' complexing agents (which may function as binder). Selected-areas electron diffraction (ED) photographs were also obtained. No any streakings are visible in the electron diffraction pattern which indicates that point or planar defects are absent in the structure of synthesized garnet.

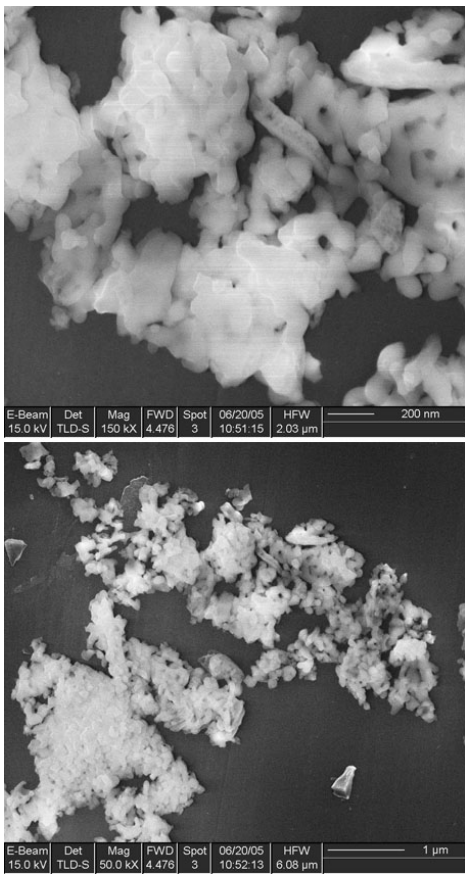


**Fig. 11.** SEM micrographs of YSGG sample sintered at 1000 °C at two magnifications: ×50000 (at bottom) and ×150000 (at top)

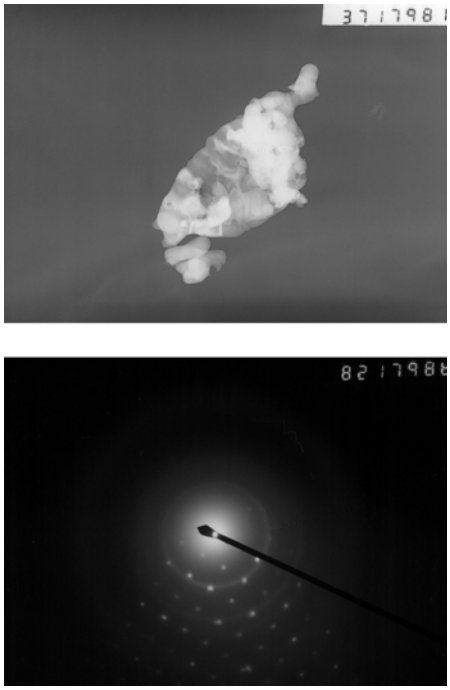

**Fig. 12.** TEM micrograph at magnification ×75000 (at top) and selected-area ED photograph (at bottom) of YSGG sample sintered at 1000 °C

The evaluated synthetic technique to YSAGG and YSGG using acetate-nitrate-glycolate intermediate illustrates the simplicity and superior potential of proposed method. This innovative approach offers a feasible way to obtain a new nanoscaled ceramic materials having garnet structure with well-established application as laser hosts. Lanthanide doped mixed-metal garnets RE:$Y_3Sc_2AlGa_2O_{12}$ (RE = Nd, Ho, Er, Tb, Dy, Yb) have been synthesized using the same aqueous sol-gel synthesis route [56]. The calcination of RE:Y-Sc-Al-Ga-O acetate-nitrate-glycolate precursor gel at 1000 °C also produced fully crystalline RE:$Y_3Sc_2AlGa_2O_{12}$ garnet phases (see Fig. 13).

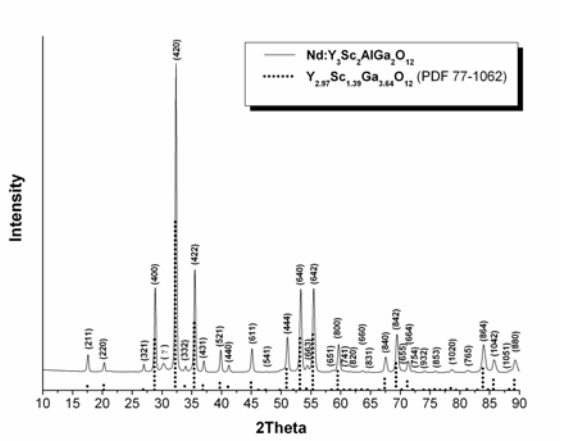


**Fig. 13.** X-ray diffraction pattern of Nd:YSAGG sample

For comparison, the XRD pattern of known $Y_{2.97}Sc_{1.39}Ga_{3.64}O_{12}$ (PDF 77-1062) is also included in Fig. 13. Thus, the XRD data confirm $Y_3Sc_2AlGa_2O_{12}$ to be the main crystalline component. All single lines are indexed, and only one unindexed line at around $2\theta \approx 30.5°$ could be observed. The SEM image of Tb:YSAGG sample calcined at 1000 °C is shown in Fig. 14. This SEM image exhibit clustered nanograins made up of several tiny crystallites with a defined structure. Individual particles seem to be nearly nano-sized crystals with an average particle size less than 50 nm.

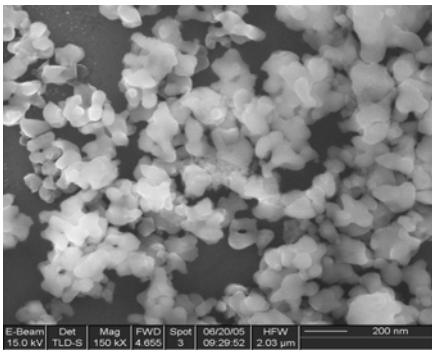


**Fig. 14.** SEM micrograph of Tb:YSAGG sample sintered at 1000°C. Magnification ×150000

It was demonstrated for the first time low-temperature synthesis (900 °C) of new mixed-metal garnets $Y_3Al_{5-x}In_xO_{12}$ [57]. The formation of $Y_3Al_{5-x}In_xO_{12}$ garnets proceeds only within narrow substitutional range. The formation of a single-phase material depends on the chemical stoichiometry in the reaction system. The increase in the indium content from x = 1.75 to x = 2.0 destabilizes the garnet phase, presumably due to the large ionic radius of $In^{3+}$. The critical value of the mean cationic radius in the octahedral positions at which the substitutional effects occur was found to be in the range of

0.631 Å – 0.644 Å, which corresponds to the chemical compositions of $Y_3Al_{3.25}In_{1.75}O_{12}$ and $Y_3Al_3In_2O_{12}$, respectively.

Since their discovery the iron-containing oxide phases with $A_3B_5O_{12}$ cubic garnet structure have been the subject of extensive investigations. These oxides possess unique magnetic, magneto-optical, thermal, electrical and mechanical properties such as ferrimagnetizm, excellent creep and radiation damage resistance, high thermal conductivity, high electrical resistivity, controllable saturation magnetization, moderate thermal expansion coefficients, energy-transfer efficiency, narrow linewidth in ferromagnetic resonance and others. Sol-gel methods based on *in-situ* generation of mixed-metal chelates by complexing metal ions with citric acid, 1,2-ethanediol or tartaric acid in an aqueous media have been elaborated to prepare iron containing garnet $Y_3Fe_5O_{12}$ (YIG) [58 – 61]. The $^{57}Fe$ Mössbauer spectrum of the $Y_3Fe_5O_{12}$ synthesized by sol-gel route is shown in Fig. 15.

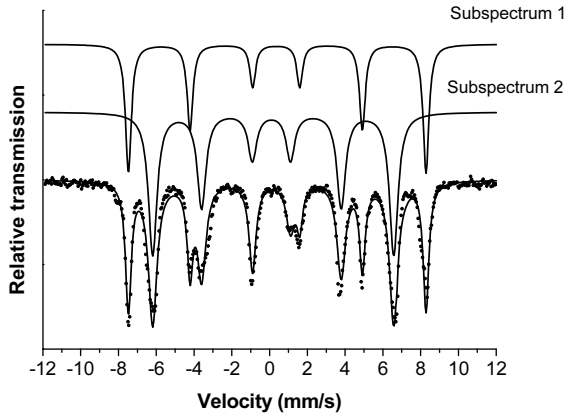


**Fig. 15.** Mössbauer spectrum of $Y_3Fe_5O_{12}$ synthesized by glycolate route.

This is a typical spectrum of single-phase yttrium iron garnet $Y_3Fe_5O_{12}$. Subspectrum 1 (sextet $Fe_2$) corresponds to the octahedral position of Fe in the garnet structure ($B_{Hf}$ = 48.9 T) and subspectrum 2 (sextet $Fe_3$) corresponds to the tetrahedral position of Fe in the garnet structure ($B_{Hf}$ = 39.6 T). Besides the hyperfine interaction parameters of these two sextets ($Fe_2$ and $Fe_3$) could be characterized by $\delta$ = (0.38 ±0.02) mm/s and $\delta$ = (0.15 ±0.01) mm/s, $\Delta$ = (0.050 ±0.004) mm/s and $\Delta$ = (0.090 ±0.003) mm/s, $\Gamma$ = (0.36 ±0.01) mm/s and $\Gamma$ = (0.62 ±0.02) mm/s, respectively. Finally, differently substituted yttrium and gadolinium iron garnets were also obtained by an aqueous sol-gel route [62 – 64].

## 6. GARNETS CONTAINING SILICON

Sol-gel combustion method employing tris(hydroxymethyl)-aminomethane as both complexing agent and fuel can be used for the fabrication of pure and lanthanide doped $Y_{3-x}Mg_2AlSi_2O_{12}$ garnet phosphors [65 – 70]. The technological approach used and charge-balanced composition of the phosphor enabled to achieve a stable single-phase structure of the double-substituted garnet. The recent articles demonstrated that garnets are suitable host lattices for investigating the impact of crystal field strength, disorder, and covalent interaction on the luminescence of an incorporated luminescent centre. It turned out that changing the composition of the garnets $(Y,Ln)_3(Al,Mg,Si)_5O_{12}$ is a powerful tool to govern the energy flow from the primarily excited state of the $[Xe]4f^2$ or $[Xe]4f^15d^1$ configuration to lower energy levels of the $[Xe]4f^2$ configuration. Therefore, the luminescence spectra of lanthanide doped garnets can be adjusted by tuning the host lattice to yield solely UV band emission, visible line emission, or both. These findings revealed that the incorporation of Mg and Si into (Y,Ln)AG or YAG reduces the band gap of the obtained host lattice.

The average crystallite size of these phosphors is in sub-micrometer range and tends to increase at elevated annealing temperatures. The cerium doped $Y_{3-x}Mg_2AlSi_2O_{12}$ phosphor exhibited a PL band peaked at about 600 nm with a record red-shift for cation-substituted YAG:Ce. The chromaticity coordinates of the YMASG:Ce phosphor are suitable for generating warm white light (CCT = 3000 K) through blending with a blue component at about 483 nm. This enables the development of partial conversion dichromatic warm-white LEDs with improved colour rendering characteristics. The emission intensity and the fluorescence decay characteristics of the YMASG:Ce phosphor are similar to those of YAG:Ce, what implies that such warm-white LEDs can have efficiency comparable to that of the conventional daylight dichromatic LEDs.

## 7. CONCLUSIONS

For the synthesis of garnet crystal structure compounds environmentally benign an aqueous sol-gel processes have been developed. The present study demonstrates the versatility of the solution method to yield monophasic garnets at low sintering temperature. In the design of complex nanoarchitectures, the main advantage of the sol-gel process is the versatility in the control of particle size, particle size distribution and arrangement of nanopores. Technologies that offer distinct technical advantages and also minimize toxicity in conventional syntheses are the most likely to be adapted in demanding fabrication schemes. An aqueous sol-gel technique may provide both of these advantages. As a result, an aqueous sol-gel process is likely to continue attracting the attention of chemists interested in designing advanced functional nanomaterials.

### *Acknowledgments*

The article was prepared under support of the European Social Fund Agency implementing measure VP1-3.1-ŠMM-05-K of the Human Resources Development Operational Programme of Lithuania 2007–2013 3rd priority "Strengthening of capacities of researchers and scientists" (project No. VP1-3.1-ŠMM-05-K-01-003)

**REFERENCES**

1. **Potdevin, A., Chadeyron, G., Boyer, D., Mahiou, R.** Influence of a Chelating Agent on Optical and Morphological Properties of YAG:$Tb^{3+}$ Phosphors Prepared by the Sol-gel Process *Journal of Sol-Gel Science and Technology* 39 2006: pp. 275 – 284.

2. **Guo, W., Cao, Y. G., Huang, Q. F., Li, J. T., Huang. J. Q., Huang, Z., Tang, F.** Fabrication and Laser Behaviours of Nd:YAG Ceramic Microchips *Journal of the European Ceramic Society* 31 2011: pp. 2241 – 2246.
3. **Yoshida, H., Tsubakimoto, K., Fujimoto, Y., Mikami, K., Fujita, H., Miyanaga, N., Nozawa, H., Yagi, H., Yanagitani, T., Nagata, Y., Kinoshita, H.** Optical Properties and Faraday Effect of Ceramic Terbium Gallium Garnet for a Room Temperature Faraday Rotator *Optics Express* 19 2011: pp. 15181 – 15187.
4. **Soares, L. E. S., Brugnera, A., Zanin, F. A. A., Santo, A. M. E., Martin, A. A.** Effects of Heating by Steam Autoclaving and Er:YAG Laser Etching on Dentin Components *Lasers in Medical Science* 26 2011: pp. 605 – 613.
5. **Brinker, C. J., Scherer, G. W.** Sol-Gel Science: The Physics and Chemistry of Sol-Gel Processing. Academic Press, London, 1990.
6. **Cushing, B. L., Kolesnichenko, V. L., O'Connor, C. J.** Recent Advances in the Liquid-phase Syntheses of Inorganic Nanoparticles *Chemical Reviews* 104 2004: pp. 3893 – 3946.
7. **Mackenzie, J. D., Bescher, E. P.** Chemical Routes in the Synthesis of Nanomaterials Using the Sol-Gel Process *Accounts of Chemical Research* 40 2007: pp. 810 – 818. http://dx.doi.org/10.1021/ar7000149
8. **O'Neil, A., Watkins, J. J.** Green Chemistry in the Microelectronics Industry *Green Chemistry* 6 2004: pp. 363 – 368.
9. **Matsui, Y., Horikawa, H., Iwasaki, M., Park, W.** Preparation of YAG:Ce Nanocrystals by an Environmentally Friendly Wet Process. Effect of Ce(3+) Concentration on Photoluminescent Property *Journal of Ceramic Processing Research* 12 2011: pp. 348 – 351.
10. **Vaqueiro, P., Lopez-Quintela, M. A.** Synthesis of Yttrium Aluminium Garnet by the Citrate Gel Process *Journal of Materials Chemistry* 8 1998: pp. 161 – 163.
11. **Veith, M., Mathur, S., Kareiva, A., Jilavi, M., Zimmer, M., Huch, V.** Low Temperature Synthesis of Nanocrystalline $Y_3Al_5O_{12}$ (YAG) and Ce-Doped $Y_3Al_5O_{12}$ via Different Sol-Gel Methods *Journal of Materials Chemistry* 9 1999: pp. 3069 – 3079. http://dx.doi.org/10.1039/a903664d
12. **Katelnikovas, A., Barkauskas, J., Ivanauskas, F., Beganskiene, A., Kareiva, A.** Aqueous Sol-Gel Synthesis Route for the Preparation of YAG: Evaluation of Sol-Gel Process by Mathematical Regression Model *Journal of Sol-Gel Science and Technology* 41 2007: pp. 193 – 201.
13. **Ivanauskas, F., Kareiva, A., Lapcun, B.** On the Modelling of Solid State Reactions. Synthesis of YAG *Journal of Mathematical Chemistry* 37 2005: pp. 365 – 376.
14. **Ivanauskas, F., Kareiva, A., Lapcun, B.** Diffusion and Reaction Rates of the Yttrium Aluminium Garnet Synthesis using Different Techniques *Journal of Mathematical Chemistry* 42 2007: pp. 191 – 199. http://dx.doi.org/10.1007/s10910-006-9092-y
15. **Ivanauskas ,F., Kareiva, A., Lapcun, B.** Computational Modelling of the YAG Synthesis *Journal of Mathematical Chemistry* 46 2009: pp. 427 – 442. http://dx.doi.org/10.1007/s10910-008-9468-2
16. **De la Rosa, E., Diaz-Torres, L. A., Salas, P., Arredondo, A., Montoya, J A., Angeles, C., Rodriguez, R. A.** Low Temperature Synthesis and Structural Characterization of Nanocrystalline YAG Prepared by a Modified Sol-Gel Method *Optical Materials* 27 2005: pp. 1793 – 1799. http://dx.doi.org/10.1016/j.optmat.2004.07.019
17. **Pullar, R. C., Taylor, M. D., Bhattacharya.** The Sintering Behaviour, Mechanical Properties and Creep Resistance of Aligned Polycrystalline Yttrium Aluminium Garnet (YAG) Fibres, Produced from an Aqueous Sol-Gel Precursor *Journal of the European Ceramic Society* 19 1999: pp. 1747 – 1758. http://dx.doi.org/10.1016/S0955-2219(98)00283-0
18. **Leleckaite, A., Jasaitis, D., Kareiva, A.** Sol-Gel Synthesis of Holmium- and Neodymium-Doped Yttrium Aluminium Garnet *Materials Science* (*Medžiagotyra*) 7 2001: pp. 225 – 229.
19. **Garskaite, E., Jasaitis, D., Kareiva, A.** Sol-Gel Preparation and Electrical Behaviour of Ln:YAG (Ln = Ce, Nd, Ho, Er) *Journal of Serbian Chemical Society* 68 2003: pp. 677 – 684. http://dx.doi.org/10.2298/JSC0309677G
20. **Garskaite, E., Jasaitis, D., Kareiva, A.** Lanthanide-Doped YAG via Sol-Gel Process: Microstructural, Electrical and Magnetic Properties *Chemija* 14 2003: pp. 89 – 93.
21. **Hreniak, D., Strek, W., Mazur, P.** Preparation, Spectroscopy and Morphology of Nd:YAG Nanostructures *Materials Science* (*Poland*) 20 2002: pp. 39 – 45.
22. **Hreniak, D., Strek, W.** Synthesis and Optical Properties of $Nd^{3+}$-Doped $Y_3Al_5O_{12}$ Nanoceramics *Journal of Alloys and Compounds* 341 2002: pp. 183 – 186. http://dx.doi.org/10.1016/S0925-8388(02)00067-1
23. **Singh, R., Khardekar, R. K., Kumar, A., Kohli, D. K.** Preparation and Characterization of Nanocrystalline Nd-YAG Powder *Materials Letters* 61 2007: pp. 921 – 924. http://dx.doi.org/10.1016/j.matlet.2006.06.013
24. **Mathur, S., Shen, H., Veith, M., Rapalaviciute, R., Agne, T.** Structural and Optical Properties of Highly Ng-Doped Yttrium Aluminum Garnet Ceramics from Alkoxide and Glycolate Precursors *Journal of the American Ceramic Society* 89 2006: pp. 2027 – 2033.
25. **Lu, C. H., Hong, H. C., Jagannathan, R.** Sol-Gel Synthesis and Photoluminescent Properties of Cerium-Ion Doped Yttrium Aluminium Garnet Powders *Journal of Materials Chemistry* 12 2002: pp. 2525 – 2530. http://dx.doi.org/10.1039/b200776m
26. **Zhou, Y., Lin, J., Yu, M., Wang, S., Zhang, H.** Synthesis-Dependent Luminescence Properties of $Y_3Al_5O_{12}$:$Re^{3+}$ (Re = Ce, Sm, Tb) Phosphors *Materials Letters* 56 2002: pp. 628 – 636. http://dx.doi.org/10.1016/S0167-577X(02)00567-0
27. **Pan, X. Y., Wu, M. M., Su, Q.** Comparative Investigation on Synthesis and Photoluminescence of YAG:Ce Phosphor *Materials Science and Engineering B* 106 2004: pp. 251 – 256. http://dx.doi.org/10.1016/j.mseb.2003.09.031
28. **Katelnikovas, A., Justel, T., Uhlich, D., Jorgensen, J.-E., Sakirzanovas, S., Kareiva, A.** Characterization of Cerium-doped Yttrium Aluminium Garnet Nanopowders Synthesized via Sol-Gel Process *Chemical Engineering Communications* 195 2008: pp. 758 – 769. http://dx.doi.org/10.1080/00986440701691194
29. **Katelnikovas, A., Vitta, P., Pobedinskas, P., Tamulaitis, G., Zukauskas, A., Jørgensen, J.-E., Kareiva, A.** Photoluminescence in Sol-Gel Derived YAG:Ce Phosphors *Journal of Crystal Growth* 304 2007: pp. 361 – 368. http://dx.doi.org/10.1016/j.jcrysgro.2007.03.006

30. **Lu, C-H., Hsu, W-T., Dhanaraj, J., Jagannathan, R.** Sol-Gel Pyrolysis and Photoluminescent Characteristics of Europium-Ion Doped Yttrium Aluminium Garnet Nanophosphors *Journal of the European Ceramic Society* 24 2004: pp. 3723 – 3729. http://dx.doi.org/10.1016/j.jeurceramsoc.2003.12.009

31. **Georgescu, S., Chinie, A. M., Stefan, A., Toma, O.** Effects of Thermal Treatment on the Luminescence of YAG:Eu Nanocrystals Synthesized by a Nitrate-Citrate Sol-Gel Method *Journal of Optoelectronics and Advanced Materials* 7 2005: pp. 2985 – 2990.

32. **Zhou, Y., Lin, J., Yu, M., Wang, S.** Comparative Study on the Luminescent Properties of $Y_3Al_5O_{12}:RE^{3+}$ (RE: Eu, Dy) Phosphors Synthesized by Three Methods *Journal of Alloys and Compounds* 375 2004: pp. 93 – 97.

33. **Leleckaite, A., Kareiva, A., Bettentrup, H., Jüstel, T., Meyer, H.-J.** Sol-Gel Preparation and Characterization of Codoped Yttrium Aluminium Garnet Powders *Zeitschrift für Anorganische und Allgemeine Chemie* 631 2005: pp. 2987 – 2993. http://dx.doi.org/10.1002/zaac.200500315

34. **Garskaite, E., Lindgren, M., Einarsrud, M.-A., Grande, T.** Luminescent Properties of Rare Earth (Er, Yb) Doped Yttrium Aluminium Garnet Thin Films and Bulk Samples Synthesized by an Aqueous Sol-Gel Technique *Journal of the European Ceramic Society* 30 2010: pp. 1707 – 1715.

35. **Leleckaite, A., Urbonaite, S., Tonsuaadu, K., Kareiva, A.** Sol-gel Synthesis and Characterization of Yttrium Gallium Garnets *Proc. SPIE (Optical Materials and Applications / Ed. A. Rosental)* 5946 2005: pp. 47 – 54.

36. **Mathur, S., Shen, H., Leleckaite, A., Beganskiene, A., Kareiva, A.** Low-Temperature Synthesis and Characterization of Yttrium-Gallium Garnet $Y_3Ga_5O_{12}$ (YGG) *Materials Research Bulletin* 40 2005: pp. 439 – 446. http://dx.doi.org/10.1016/j.materresbull.2004.12.002

37. **Katelnikovas, A., Kareiva, A.** Low-Temperature Synthesis of Lutetium Gallium Garnet (LGG) using Sol-Gel Technique *Materials Letters* 62 2008: pp. 1655 – 1658. http://dx.doi.org/10.1016/j.matlet.2007.09.053

38. **Garskaite, E., Dubnikova, N., Katelnikovas, A., Pinkas, J., Kareiva, A.** Syntheses and Characterisation of $Gd_3Al_5O_{12}$ and $La_3Al_5O_{12}$ Garnets *Collection of Czechoslovak Chemical Communications* 72 2007: pp. 321 – 333. http://dx.doi.org/10.1135/cccc20070321

39. **Saxena, S., Asokkumar, A. K., Lal, B.** Citrate-Nitrate Route for the Synthesis and Characterization of TAG using Sol-Gel Techniques *Journal of Sol-Gel Science and Technology* 41 2007: pp. 245 – 248. http://dx.doi.org/10.1007/s10971-006-1503-9

40. **Zhong, Y. R., Yu, R. S., Li, Z. X., Wang, B. Y., Wei, L.** Luminescence and Defect Study of $Ce^{3+}$-Doped $Lu_3Al_5O_{12}$ *Phosphors Materials Science Forum* 607 2009: pp. 128 – 130. http://dx.doi.org/10.4028/www.scientific.net/MSF.607.128

41. **Dubnikova, N., Garskaite, E., Pinkas, J., Bezdicka, P., Beganskiene, A., Kareiva, A.** Sol-Gel Preparation of Selected Lanthanide Aluminium Garnets *Journal of Sol-Gel Science and Technology* 55 2010: pp. 213 – 219.

42. **Dubnikova, N., Garskaite, E., Beganskiene, A., Kareiva, A.** Sol-Gel Synthesis and Characterization of Sub-Microsized Lanthanide (Ho, Tm, Yb, Lu) Aluminium Garnets *Optical Materials* 33 2011: pp. 1179 – 1184.

43. **Leleckaite, A., Jasaitis, D., Salkus, B., Sadunas, A., Kareiva, A.** Scanning Electron Microscopy – a Powerful Tool for the Characterization of Materials. 3. Sol-Gel Synthesis of Lanthanum-Aluminium Garnet *Environmental Chemistry and Physics* 25 2003: pp. 143 – 147.

44. **Lipinska, L., Lojko, L., Klos, A., Ganschow, S., Diduszko, R., Ryba-Romanowski, W., Pajaczkowska, A.** Nanopowders and Crystals in $(Y_{1-x}Nd_x)_3Al_5O_{12}$ System: Preparation and Properties *Journal of Alloys and Compounds* 432 2007: pp. 177 – 182. http://dx.doi.org/10.1016/j.jallcom.2006.05.112

45. **Garskaite, E., Sakirzanovas, S., Kareiva, A., Glaser, J., Meyer, H.-J.** Synthesis and Structure of Europium Aluminium Garnet (EAG) *Zeitschrift für Anorganische und Allgemeine Chemie* 633 2007: pp. 990 – 993. http://dx.doi.org/10.1002/zaac.200700027

46. **Muliuoliene, I., Jasaitis, D., Kareiva, A.** Sol-Gel Synthesis and Characterization of Mixed-Metal Garnet *Journal of Materials Science and Technology* 9 2001: pp. 142 – 152.

47. **Jasaitis, D., Muliuoliene, I., Sivakov, V., Shen, H., Rapalaviciute, R., Mathur, S., Kareiva, A.** From Precursors to Ceramic Materials. 1. Sol-Gel Chemistry Approach in the Preparation of Precursors for the Advanced Optical Materials *Materials Science* (*Medžiagotyra*) 8 2002: pp. 156 – 160.

48. **Muliuoliene, I., Jasaitis, D., Siuksciuviene, Z., Salkus, B., Kazlauskas, R., Kareiva, A.** Fabrication from Sol-Gel Precursor and X-ray Powder Diffraction Analysis Study of New Mixed-Metal Garnet *Environmental Chemistry and Physics* 24 2002: pp. 18 – 24.

49. **Muliuoliene, I., Jasaitis, D., Kareiva, A., Blaschkowski, B., Glaser, J., Meyer, H.-J.** Sol-Gel Synthesis and Characterization of Mixed-Metal Garnet $Y_3ScAl_3GaO_{12}$ (YSAGG) *Journal of Materials Science Letters* 22 2003: pp. 349 – 351. http://dx.doi.org/10.1023/A:1022636924815

50. **Muliuoliene, I., Mathur, S., Jasaitis, D., Shen, H., Sivakov, V., Rapalaviciute, R., Beganskiene, A., Kareiva, A.** Evidence of the Formation of Mixed-Metal Garnets via Sol-Gel Synthesis *Optical Materials* 22 2003: pp. 241 – 250. http://dx.doi.org/10.1016/S0925-3467(02)00271-9

51. **Pakutinskiene, I., Mathur, S., Shen, H., Kudabiene, G., Jasaitis, D., Kareiva, A.** From Precursors to Ceramic Materials. II. Synthesis and Specific Features of New Garnet Structure Compounds *Materials Science* (*Medžiagotyra*) 9 2003: pp. 374 – 378.

52. **Leleckaite, A., Kareiva, A.** Synthesis of Garnet Structure Compounds using Aqueous Sol-Gel Processing *Optical Materials* 26 2004: pp. 123 – 128. http://dx.doi.org/10.1016/j.optmat.2003.11.009

53. **Garskaite, E., Moravec, Z., Pinkas, J., Mathur, S., Kazlauskas, R., Kareiva, A.** Synthesis and Evolution of Crystalline Garnet Phases in $Y_3Sc_{5-x}Ga_xO_{12}$ *Philosophical Magazine Letters* 85 2005: pp. 557 – 562. http://dx.doi.org/10.1080/09500830500398389

54. **Pinkas, J., Garskaite, E., Beganskiene, A., Nenartaviciene, G., Kareiva, A.** Influence of Annealing Temperature on the Phase Purity, Crystallinity and Optical Properties of $Y_3Sc_2Ga_3O_{12}$ Prepared by Different Methods *Chemija* 4 2006: pp. 56 – 60.

55. **Sakirzanovas, S., Sun, L., Yan, Ch., Kareiva, A.** Sol-Gel Synthesis of Nanosized $Y_3Sc_{2.5}Ga_{2.5}O_{12}$ Garnet *Mendeleev Communications* 18 2008: pp. 251 – 252. http://dx.doi.org/10.1016/j.mencom.2008.09.007

56. **Sakirzanovas, S., Kareiva, A.** Sol-Gel Synthesis of Nanosized Lanthanide-Doped Mixed-Metal Garnets *Lithuanian Journal of Physics* 47 2007: pp. 75 – 80.

57. **Skaudzius, R., Selskis, A., Pinkas, J., Kareiva, A.** Synthesis and Evolution of Crystalline Garnet Phases in $Y_3Al_{5-x}In_xO_{12}$ *Journal of Physics: Conference Series* 93 2007: p. 012003.

58. **Vaqueiro, P., Lopez-Quintela, M. A.** Influence of Complexing Agents and pH on Yttrium-Iron Garnet Synthesized by the Sol-Gel Method *Chemistry of Materials* 9 1997: pp. 2836 – 2841. http://dx.doi.org/10.1021/cm970165f

59. **Sanchez, R. D. Rivas, J., Vaqueiro, P., Lopez-Quintela, M. A., Caeiro, D.** Particle Size Effects on the Properties of Magnetic Yttrium Iron Garnets Prepared by a Sol-Gel Method *Journal of Magnetism and Magnetic Materials* 247 2002: pp. 92 – 98.

60. **Vajargah, S. H., Hosseini, H. R. M., Nemati, Z. A.** Synthesis of Nanocrystalline Yttrium Iron Garnets by Sol-Gel Combustion Process: The Influence of pH of Precursor Solution *Materials Science and Engineering B* 129 2006: pp. 211 – 215.

61. **Garskaite, E., Gibson, K., Leleckaite, A., Glaser, J., Niznansky, D., Kareiva, A., Meyer, H.-J.** On the Synthesis and Characterization of Iron-Containing Garnets ($Y_3Fe_5O_{12}$, YIG and $Fe_3Al_5O_{12}$, IAG) *Chemical Physics* 323 2006: pp. 204 – 210. http://dx.doi.org/10.1016/j.chemphys.2005.08.055

62. **Matsumoto, K., Yamaguchi, K., Fujii, T., Ueno, A.** Preparation of Bismuth-Substituted Yttrium-Iron-Garnet Powders by the Citrate Gel Process *Journal of Applied Physics* 69 1991: pp. 5918 – 5920.

63. **Grasset, F., Mornet, S., Demourgues, A., Portier, J., Bonnet, J., Vekris, A., Duguet, E.** Synthesis, Magnetic Properties, Surface Modification and Cytotoxicity Evaluation of $Y_3Fe_{5-x}Al_xO_{12}$ ($0 \le x \le 2$) Garnet Submicron Particles for Biomedical Applications *Journal of Magnetism and Magnetic Materials* 234 2001: pp. 409 – 418.

64. **Dong, B., Cui, Y. M., Yang, H., Yu, L. X., Jin, W. Q., Feng, S. H.** The Preparation and Magnetic Properties of $Gd_xBiY_{2-x}Fe_5O_{12}$ Nanoparticles *Materials Letters* 60 2006: pp. 2094 – 2097. http://dx.doi.org/10.1016/j.matlet.2005.12.143

65. **Katelnikovas, A., Bettentrup, H., Uhlich, D., Sakirzanovas, S., Justel, T., Kareiva, A.** Synthesis and Optical Properties of $Ce^{3+}$-Doped $Y_3Mg_2AlSi_2O_{12}$ Phosphors *Journal of Luminescence* 129 2009: pp. 1356 – 1361. http://dx.doi.org/10.1016/j.jlumin.2009.07.006

66. **Katelnikovas, A., Bareika, T., Vitta, P., Justel, T., Winkler, H., Kareiva, A., Zukauskas, A., Tamulaitis, G.** $Y_{3-x}Mg_2AlSi_2O_{12}:Ce_x^{3+}$ Phosphors – Prospective for Warm-White Light Emitting Diodes *Optical Materials* 32 2010: pp. 1261 – 1265. http://dx.doi.org/10.1016/j.optmat.2010.04.031

67. **Katelnikovas, A., Ogieglo, J. M., Winkler, H., Kareiva, A., Jüstel, T.** Synthesis of $Y_{3-x}Lu_xAl_3MgSiO_{12}$ Garnet Powders by Sol-Gel Method *Journal of Sol-Gel Science and Technology* 59 2011: pp. 311 – 314. http://dx.doi.org/10.1007/s10971-011-2502-z

68. **Katelnikovas, A., Bettentrup, H., Dutczak, D., Kareiva, A., Jüstel, T.** On the Correlation between the Composition of $Pr^{3+}$ Doped Garnet Type Materials and Their Photoluminescence Properties *Journal of Luminescence* 131 2011: pp. 2754 – 2761.

69. **Katelnikovas, A., Winkler, H., Kareiva, A., Jüstel, T.** Synthesis and Optical Properties of Green to Orange Tunable Garnet Phosphors for pcLEDs *Optical Materials* 33 2011: pp. 992 – 995. http://dx.doi.org/10.1016/j.optmat.2010.11.023

70. **Katelnikovas, A., Jurkevicius, J., Kazlauskas, K., Vitta, P., Jüstel, T., Kareiva, A., Zukauskas, A., Tamulaitis, G.** Efficient Cerium-Based Sol-Gel Derived Phosphors in Different Garnet Matrices for Light-Emitting Diodes *Journal of Alloys and Compounds* 509 2011: pp. 6247 – 6251. http://dx.doi.org/10.1016/j.jallcom.2011.03.032